

# Three-dimensional terahertz pulse imaging of dental tissue

**David Crawley**, MEMBER SPIE

University of Cambridge  
Cavendish Laboratory  
Cambridge, United Kingdom  
and  
Tera View Limited  
Cambridge Science Park  
Cambridge, United Kingdom

**Christopher Longbottom**, MEMBER SPIE

University of Dundee  
Dundee Dental School  
Park Place, Dundee  
United Kingdom

**Vincent P. Wallace**, MEMBER SPIE

**Bryan Cole**

**Don Arnone**, MEMBER SPIE

Tera View Limited  
Cambridge Science Park  
Cambridge, United Kingdom

**Michael Pepper**

University of Cambridge  
Cavendish Laboratory  
Cambridge, United Kingdom  
and  
Tera View Limited  
Cambridge Science Park  
Cambridge, United Kingdom

## 1 Introduction

There are a number of clinical problems that cannot be resolved with only a simple planar transmission or reflection image. Imaging teeth structures is one such problem. A normal tooth will have a layer of highly mineralized enamel surrounding dentine (which is less mineralized) with a soft tissue pulp in the center. In some cases, such as in the analysis of enamel erosion in dentistry, there is no current technology that can provide adequate 3-D images in a practical way.<sup>1</sup> Nondestructive measurements are required to characterize enamel erosion, an increasing public health problem.<sup>2,3</sup> We present a technique that can be used to image enamel thickness for anterior teeth. We outline a quasi-3-D imaging system that uses pulsed terahertz (THz= $10^{12}$  Hz) radiation and present data from experiments applying the system to dental imaging. THz is a form of electromagnetic radiation located between microwave and infrared frequencies.<sup>4</sup> A number of systems capable of characterizing an object to generate a 2-D image have appeared<sup>5–7</sup> and methods for imaging biological tissues in 2-D using THz radiation have recently been developed.<sup>8,9</sup> Terahertz pulse imaging (TPI) is capable of distinguishing between different dental tissues.<sup>4,10</sup> In particular with THz radiation, there is a refractive index change between the tissues that make up different layers in teeth.<sup>10</sup> This gives rise to the interesting possibility of reflecting THz pulses off the dielectric layers in the tooth to gather 3-D information. This work was preceded by research to conduct ranging<sup>11</sup> of thin plastic

**Abstract.** There are unresolved clinical problems that require the provision of accurate 3-D images of tissue structures such as teeth. In particular, measurements of dental enamel thickness are necessary to quantify problems associated with enamel erosion, yet currently there is no nondestructive method to obtain this information. We present a method that relies on the use of pulsed terahertz radiation to gain 3-D information from dental tissues. We discuss results from 14 samples and demonstrate that we can reliably and accurately quantify enamel thickness. We show that in a series of 22 surfaces, we can image pertinent subsurface features 91% of the time. Example images are shown where structures in teeth at depth are rendered accurate to within 10  $\mu\text{m}$ . We discuss issues that arise using this imaging method and propose ways in which it could be used in clinical practice.  
© 2003 Society of Photo-Optical Instrumentation Engineers. [DOI: 10.1117/1.1559059]

Keywords: terahertz pulse imaging; dental tissue; enamel erosion.

Paper 02013 received Mar. 1, 2002; revised manuscript received Sep. 16, 2002; accepted for publication Oct. 7, 2002.

objects as well as proposals to use THz technology for high frequency radar.<sup>12</sup> This work reports preliminary trials of quasi-3-D THz imaging on *in vitro* samples of teeth. Our current system requires 3 min/scan. This methodology has been applied to dental imaging but the technique can, in principal, be applied to a broad range of 3-D bioimaging applications.

## 2 Materials and Methods

A TPI system was used in reflection geometry, which is shown in Fig. 1. An amplified, ultrafast laser system (RegA 9000, Coherent Incorporated, Santa Clara, California) generates a train of 250-fs laser pulses with a repetition rate of around 250 kHz that are split into a pump and a probe beam. The pump beam drives the THz source, which is a 1-mm-wide aperture antenna, fabricated using lithographic deposition of nickel chromium and then gold onto a 1-mm-thick high resistivity GaAs wafer. The operational details of wide aperture antennas have been described elsewhere.<sup>13,14</sup> An anticorona lacquer was used to help eliminate sparking across this gap. The device was typically biased between 500 and 1000 V DC. The emitted THz pulses passed through a series of off-axis paraboloid mirrors and were focused onto the sample, which was mounted on a stationary stand; the angle of reflection was 30 deg to normal incidence. The optics were scanned in the  $x$  and  $y$  plane to acquire the image. The reflected THz pulses

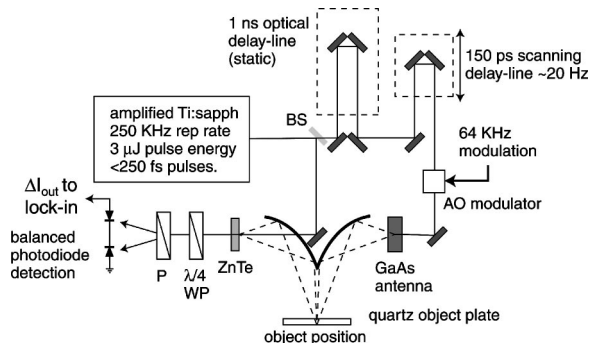


**Fig. 1** A schematic of the TPI system used. The solid line represents the NIR beam while the broken line indicates the THz path. Shaded boxes indicate mirrors, and generation and detection crystals. Abbreviations: BS is the beam splitter, P is the polarizer, and  $\lambda/4$  WP is the quarter waveplate.

were recollimated using another pair of off-axis paraboloid mirrors and focused onto a 1-mm-thick zinc telluride (ZnTe) crystal, colinearly with the NIR probe beam. Detection was achieved using the linear electro-optic Pockel's effect. The THz radiation induces a birefringence in the ZnTe crystal, and the polarization of the probe beam is modified from planar to elliptical, giving a nonzero output current from the balanced photodiodes. Because the effect is linear and is assumed to be instantaneous, the output current is directly proportional to the THz electric field. To improve the sensitivity, the pump beam was chopped at a quarter of the laser repetition rate with an acousto-optic modulator so that lock-in detection of the photodiode difference current could be used. This modulator was synchronized with the laser pulse to avoid unwanted beat effects in our images. By sweeping an optical delay through the entire THz pulse, time and depth information was obtained.

There were two delay stages in our setup. One provides for broad synchronization of the path length between the pump and probe beam. The other is a delay line that oscillates at 20 Hz and sweeps in the time domain to allow a complete THz pulse to be sampled. Part of the incident THz pulse reflects from the tooth surface. The rest passes into the sample and reflects off the dielectric interfaces within the sample. The delay line oscillates at a speed much greater than the movement of the stages and thus allows several complete THz waveforms to be captured at each point, averaged, and recorded using a computer with a fast analogue-to-digital converter. The amplitude of the oscillating delay line can be altered depending on the length of the THz pulse one wishes to measure or the depth into the sample one would like to probe. It is usual to image to a depth of around 1 mm into the tooth. Enamel tissue has a refractive index of approximately 3, giving an optical path length of 3 mm. Typically, the amplitude of the oscillating delay line is set to 6 mm to ensure complete capture of all relevant frequency components.

After generation, the THz pulse contains some ringing, secondary spikes, and other features from imperfections in the optics and the particular wavelengths generated. When trying to use these pulses to generate images in an ultrasound-like b-scan mode (cross section through the object), these features introduce confusing secondary lines and other artefacts. It is possible to process the data to generate clearer images that are

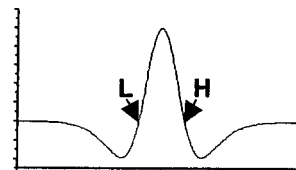


**Fig. 2** The shape of our double Gaussian filter. *L* and *H* indicate the high- and low-pass filter points of the filter that are the only operator-specified parameters.

easier to understand. Because the incident pulse contains artefacts, the pulses that are returned from the dielectric interfaces would be expected to contain a similar structure. By Fourier deconvolving the reflected pulse with a previously measured example of the input pulse, it is possible to reduce the artefacts associated with this structure. To further improve the signal-to-noise ratio, we apply a numerical filter to our data prior to the second Fourier transform in our deconvolution. It is important to note that dielectric interfaces take on the shape of the Fourier transform of the filter. The specific filter chosen was a double Gaussian of the form:

$$F(x) = de^{-(x-\gamma)^2/c^2} - ce^{-(x-\gamma)^2/d^2},$$

where  $x$  is the measurement in the frequency domain, and  $c$ ,  $d$  and  $\gamma$  are parameters that are defined implicitly from the two operator input parameters of the high- and low-pass edges of the filter (indicated by *H* and *L* on Fig. 2).

The Fourier transform of this filter shape is another double Gaussian and all dielectric interfaces imaged will take on its shape. For example, in a given image a positive change in refractive index may appear as a light line bordered by two dark lines, while a negative change in refractive index will appear as a dark line bordered by two light lines. All data were acquired and processed with programs developed in-house using LabVIEW (National Instruments, Texas), which allows any lateral or transverse sections of data to be viewed to find appropriate diagnostic information.

In making the determination as to whether an interface was resolved, the image was initially examined visually and then the pulse for the interface (which would take on a double Gaussian shape) was examined. Only if the pulse was at least three times as high as the associated background noise for that trace would the interface be considered resolved.

### 2.1 Samples

Human incisors were used for this study. It is expected that in clinical studies of enamel erosion, incisors would be the teeth used, because they are relatively easy to access. Further, incisors tend to be less highly curved and have thinner enamel layers, which make them more suitable for use in our imaging system. The teeth used in the study were supplied by the University of Dundee Dental School and were chosen from a pooled sample, collected throughout Scotland, with the informed consent of those from whom they were extracted. The Dental School obtains consent for the use of such teeth in accordance with pertaining national and local ethics committee guidelines. As with all teeth, there was a layer of high

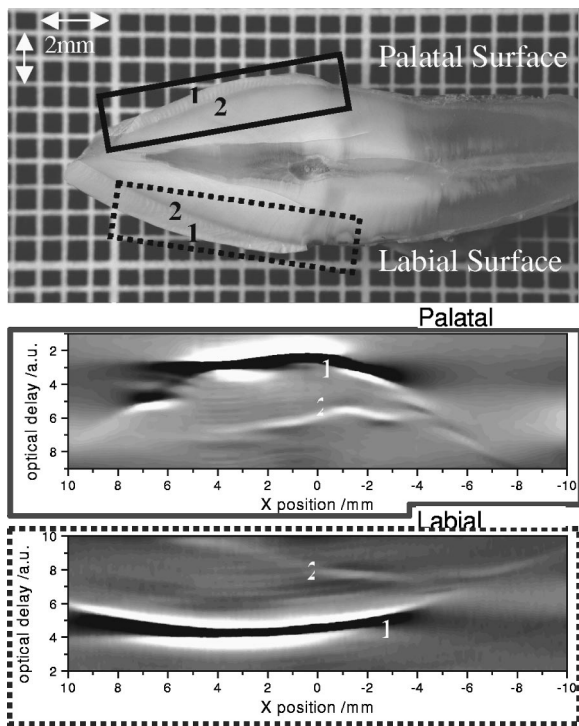


**Fig. 3** A visible image of a section of a human incisor (top) and the corresponding THz images: 1. enamel air interface, and 2. enamel dentine interface.

refractive index enamel covering lower refractive index dentine. A measurement from the enamel surface to the enamel-dentine junction gives the enamel thickness.

A pilot experiment with a single hemisected human incisor was followed by a more extensive series of 12 hemisected teeth. To confirm that our technique could produce quantitatively accurate results, an additional sample was measured. This was of a whole incisor tooth, the labial enamel thickness of which had been artificially altered to produce a series of linear “steps” in a mesio-distal direction, by sequentially acid etching (for 2 min) with a proprietary etching gel, washing with water, and subsequently polishing using a rotating rubber cup with prophylaxis paste. Each step was constructed to be 100  $\mu\text{m}$  deeper than the next.

### 3 Results

In an initial attempt to measure enamel thickness, a pilot human incisor was examined. This sample was cut in half to allow comparison of the THz and visible image. The tooth in Fig. 3 was imaged on both the front (labial) and the rear (palatal) surfaces. The curvature of all tooth surfaces is exaggerated on the THz image. This is because dental tissue has a larger refractive index than air, thus the transit times for the THz pulse is longer in dental tissue and the surface appears more curved. The enamel-dentine interface is light on dark, whereas the enamel-air interface is dark on light. This is because the change in refractive index from air to enamel is positive, whereas the change in refractive index from enamel to dentine is negative. The enamel-dentine junction is also

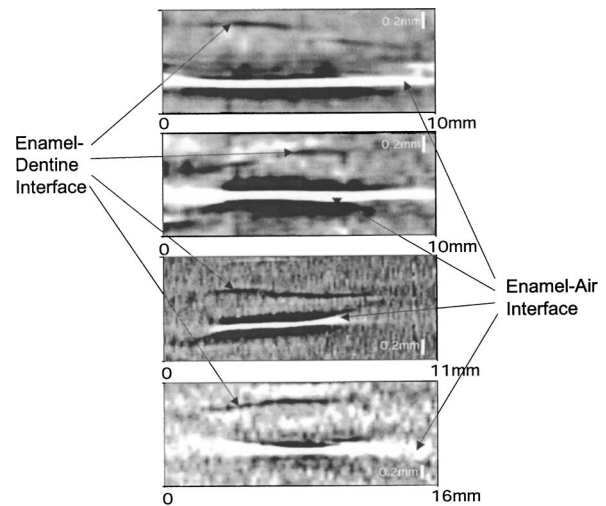


**Fig. 4** Four example images from the set of 12 dental samples showing the enamel air interfaces and the enamel dentine interfaces.

less pronounced than the enamel-air interface for two reasons: the refractive index change is smaller and the THz pulse is attenuated on passing through the enamel.

A larger set of 12 incisors was also imaged in this way. 22 surfaces were examined (two had enamel that was clearly too thick and curved to be well imaged) and the enamel dentine junction was resolved in 20 cases (91%). Example images are shown in Fig. 4. In all four THz images, the enamel dentine junction is clearly visible as a dark line against a lighter background, with the enamel-air interface being a light line against a darker background. The enamel thickness in the images was between 0.4 and 0.9 mm. The signal-to-noise ratio from the enamel dentine junction in an example pixel in the uppermost image was measured to be 14.3. We were also able to image dental samples that had the surface altered artificially. These samples had steps on the surface, the difference in height between the steps was typically 100  $\mu\text{m}$ .

Figure 5 shows an image of a whole incisor tooth, the labial enamel thickness of which had been artificially altered to produce a series of linear steps in a mesio-distal direction (schematically shown in Fig. 5(b)). Each step is 100  $\mu\text{m}$  deeper than the next. All our TPI measurements are within 10  $\mu\text{m}$  of the distances one would naively assume. This is in excellent agreement with our expected systematic errors. Note that the image of the surface of the tooth (the thick white line bordered by two dark lines) appears relatively smooth when compared with the enamel dentine junction (the darker lines further up the image), which seems to consist of a series of steps. However, the enamel dentine junction was not affected by the treatment of the surface of the tooth and would be expected to be continuous and smooth. The thicknesses indicated in this image are determined by making assumptions about the refractive index of the dental tissue. Previous investigations<sup>10,15</sup> indicate that the refractive index of enamel dental tissue is largely constant between subjects with the index  $3.1 \pm 0.22$ . Because the refractive index ( $n$ ) of the enamel is 3.1 times that of air ( $n = 1$ ), the time of flight of the THz pulse from the air-enamel interface to the enamel-dentine junction is therefore 3.1 times longer the equivalent path in

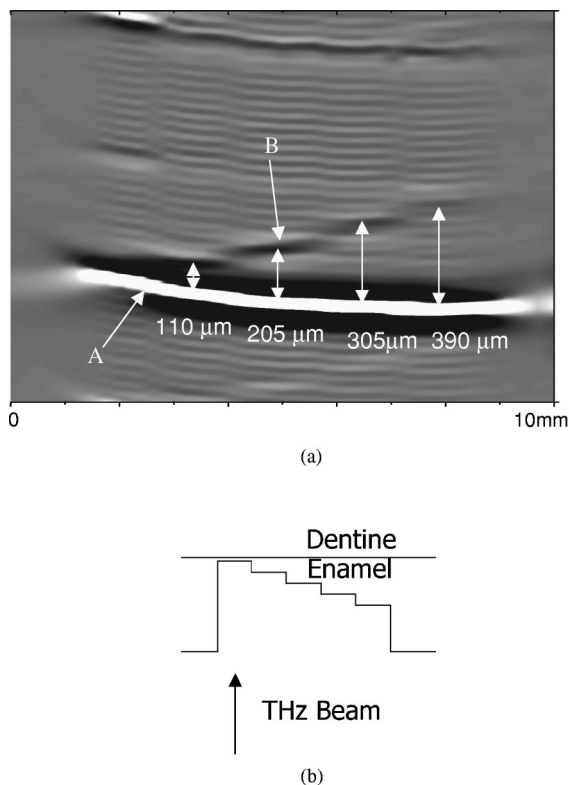


**Fig. 5** (a) An image of a whole human incisor with steps etched into the surface. The enamel air interface as represented by a thick white line is indicated (A). Portions of the enamel dentine junction are indicated (B). The thickness ( $\mu\text{m}$ ) of the enamel at each of the artificially induced steps as measured by TPI is indicated. (b) A schematic of the tooth.

air. This is why the surface of the enamel appears to have only small steps that are barely perceptible, while the enamel dentine junction exhibits the larger steps.

#### 4 Discussion

There are a number of issues that are being addressed to make *in vivo* measurements possible. The generation and detection crystals are both 1 mm thick and are made from high ( $\sim 3$ ) refractive index ( $n_c$ ) material. As such, the THz pulse will reflect inside these crystals and generate an echo pulse. This can be clearly seen in Fig. 5. The echo pulse will occur at a distance  $2n_c$  away from the initial pulse. When this artifact pulse is reflected in some unknown object, its properties will change in a way that is different to the initial pulse. Hence a simple deconvolution will not eliminate this pulse. Further, there will also be an artifact pulse generated in the detection crystal. These artifact pulses will overlap and a simple deconvolution will not be able to eliminate them. Further, the high refractive index of the tooth means that the angle for total internal reflection is around 17 deg. It is thus very difficult using this technique to image surfaces internal to the tooth that are at an angle greater than 17 deg to the surface of the tooth, as any THz that is reflected from this surface will not be able to find its way out of the tooth for detection. It is these two problems that made it difficult to see the enamel dentine junction, where the enamel is greater than the thickness of the

detection and generation crystals (1 mm) or where the enamel dentine junction was at an angle to the tooth surface. These two effects are the likely cause of the two failures to image the enamel dentine junction. It should be noted that these are not fundamental limitations, but merely features of our prototype experimental system. Thicker detection and generation crystals would allow the measurement of thicker samples. In clinical practice one would use a probe that could be applied to the teeth in the mouth. Such probes are currently under development in our lab. These probes would allow for the application of index matching systems on the tooth, and because the generation and detection crystals would themselves be index matched, they would avoid the problems of artefacts at the crystal thickness. Thus we expect it to be possible to reliably measure enamel thickness by this method, even where the enamel thickness is great.

To deal with random errors it might be possible, in principle, to fit a double Gaussian to our data lines and then use the accuracy, with which the double Gaussian is fitted, to determine the position of the features in our images. This method assumes that dispersion is not significant. This depends on having an output waveform that is dependably a double Gaussian. Given this, the most robust measurement of the pulse position can be made by determining the point of maximum intensity. Our ADC digitizes 2048 points, which are spread out over a distance of roughly 2 mm in a dental sample. Thus the accuracy with which the position of the peak may be determined would be  $\pm 1 \mu\text{m}$ . A thickness measurement requires the measurement of two peaks, adding in quadrature gives a combined random error of  $\pm 1.4 \mu\text{m}$ . Our system is in itself very precise as it simply measures optical path length, however, we should consider the systematic errors, which, as we shall see, are the true limiting factor for absolute thickness measurement.

Our current calibration technique relies on the artifact that is evident from the reflection of the THz within the detection and emission crystals. This artifact should occur at a distance:

$$d = \frac{n_c t_c}{n_s},$$

where  $n_c$  and  $n_s$  are the refractive indexes of the crystal and the sample, respectively, and  $t_c$  is the thickness of the crystal. The thickness of the crystal is well characterized. The refractive indices are, however, a source of error, particularly as they vary with frequency. Any error in determining the calibration will mean that there will be a systematic offset in our results. We should consider the following systematic errors. Previous measurements indicate that there is similarity between the refractive index of human dental samples, with a deviation in the refractive index of human enamel of approximately  $\pm 7\%$ . Thus absolute measurements of enamel thickness would be within this margin of error. Errors will also arise from limitations in our ability to determine the calibration thickness. These will typically be similar to those analyzed for random errors and stand at  $\pm 1.4 \mu\text{m}$ . There will be other errors arising from an inability to accurately measure the thickness and the refractive index of the crystal, which form the basis of our calibration. From the accuracy, with which it is possible to determine other features of our crystals, the nominal error is likely to be  $\pm 5\%$ . Thus total systematic

errors would be  $\pm 8.6\%$ ; for a measurement of a 0.5-mm-thick region of enamel, this corresponds to  $\pm 43 \mu\text{m}$ . However, it should be noted that in clinical practice a system such as this would be used to monitor the changes in enamel thickness rather than make an absolute measurement of enamel thickness. Thus the systematic error is of less significance. In any case, if there is an application where absolute measurements are important, attempts could be made to use *in situ* refractive index determination methods.<sup>5</sup>

To make use of THz technology in clinical practice would require a probe that could be used in the mouth. The probe would have a refractive index that is closer to that of the tooth than air. This probe would be pressed against the dental tissue one wished to measure and thus reduce the problem of total internal reflection in our measurements.

## 5 Conclusions

We have described a TPI system that can be used to generate images of dental tissue in 3-D. We have presented data from a sample of teeth, including a series of 12 human incisors, in which we were able to detect the enamel dentine junction in 91% of the cases. We have also imaged artificially altered enamel thickness to within  $10 \mu\text{m}$  of the expected results. We have thus demonstrated that we can accurately and reliably make direct measurements of enamel thickness, a technology that is necessary to monitor enamel erosion, a common dental disorder. The current system has difficulty in imaging very thick samples and in measuring angular surfaces. Future advances would require the development of a probe that can be used *in vivo*. This would allow for the probe head to be pressed against the dental hard tissue and thus to reduce the problem of total internal reflection in the tooth.

### Acknowledgments

Teraview Limited, Cambridge University's reserve award funding body, and Cambridge University's Semiconductor Physics Group have all supported this research.

## References

1. M. Addy, G. Embery, W. Edgar, and R. Orchardson, *Tooth Wear and Sensitivity*, p. 111, Martin Dunitz Ltd., London (2000).
2. A. Milosevic, P. Young, and M. Lennon, "The prevalence of tooth wear in 14 year old school children in Liverpool," *Community Dent. Health* **11**, 83–86 (1993).
3. A. Millward, L. Shaw, and A. Smith, "Continuous intra-oral pH monitoring after consumption of acidic beverages," *J. Dent. Res.* **73**, abstract no 389.
4. D. Arnone and C. Ciesla, "Applications of terahertz technology to medical imaging," *Proc. SPIE* **3828**, 209–219 (1999).
5. S. Hunsche, D. Mittleman, M. Koch, and M. Nuss, "New dimensions in T-ray imaging," *IEICE Trans. Electron.* **E81C**(2), 269–276 (1998).
6. M. Herrmann, M. Tani, and K. Sakai, "Display modes in time-resolved terahertz imaging," *Jpn. J. Appl. Phys., Part 1* **39**(11), 6254–6258 (2000).
7. Z. P. Jiang and X. C. Zhang, "Terahertz imaging via electro-optic effect," *IEEE Trans. Microwave Theory Tech.* **47**(12), 2644–2650 (1999).
8. B. Cole, R. Woodward, D. Crawley, V. Wallace, D. Arnone, and M. Pepper, "Terahertz imaging and spectroscopy of human skin *in vivo*," *Proc. SPIE* **4276**, 1–10 (2001).
9. R. Woodward, B. Cole, V. Wallace, D. Arnone, E. Linfield, and M. Pepper, "Terahertz pulse imaging of *in vitro* basal cell carcinoma samples," in *OSA Trends in Optics and Photonics (TOPS)*, **56**, 329–330 (2001).
10. D. A. Crawley, C. Longbottom, B. E. Cole, C. M. Ciesla, D. Arnone, V. P. Wallace, and M. Pepper "Terahertz pulse imaging—Potential applications in dentistry," (submitted for publication).
11. D. Mittleman, S. Hunsche, L. Boivin, and M. Nuss, "T-ray tomography," *Opt. Lett.* **22**(12), 904–906 (1997).
12. N. Froberg, M. Mack, B. B. Hu, X. C. Zhang, and D. H. Auston, "500 Ghz electrically steerable photoconducting antenna-array," *Appl. Phys. Lett.* **58**(5), 446–448 (1991).
13. J. Darrow, B. Hu, X. Zhang, and D. Auston, "Sub-picoseconds electromagnetic pulses from large-aperture photoconducting antennas," *Opt. Lett.* **15**(6), 323–325 (1990).
14. G. Mouret, W. Chen, D. Boucher, R. Bocquet, P. Mounaix, D. Theron, and D. Lippens, "High-power terahertz radiation from a high repetition-rate large-aperture photoconducting antenna," *Microwave Opt. Technol. Lett.* **17**(1), 23–27 (1998).
15. C. Ciesla, D. Arnone, A. Corchia, D. Crawley, C. Longbottom, E. Linfield, and M. Pepper, "Biomedical applications of terahertz pulse imaging," *Proc. SPIE* **3934**, 73–81 (2000).